

# Deeply Virtual Compton Scattering at HERA - A Probe of Asymptotia

L.L.Frankfurt<sup>a</sup>, A.Freund<sup>b</sup>, M. Strikman<sup>b</sup>

<sup>a</sup>*Physics Department, Tel Aviv University, Tel Aviv, Israel*

<sup>b</sup>*Department of Physics, Penn State University*

*University Park, PA 16802, U.S.A.*

## Abstract

We demonstrate that the measurement of an azimuthal angle asymmetry in deeply virtual Compton scattering (DVCS) at HERA energies, is experimentally feasible and allows one to determine for the first time the ratio,  $\eta$ , of the real to imaginary part of the DIS amplitude. We further show that such measurements would discriminate between different scenarios for the energy dependence of  $F_2(x, Q^2)$  at energies beyond those reachable at HERA.

## I. INTRODUCTION

It is generally agreed that the  $x$ -range currently available at HERA is not sufficient to test the current ideas about the onset of asymptotia via measurements of the parton densities. Therefore, the aim of this paper is to draw attention to the fact that the derivative of parton distributions with respect to  $\ln x$ , which can be measured at HERA, is rather sensitive to the asymptotic behaviour of parton densities at  $x \rightarrow 0$  which can be probed at the LHC only. Actually, the experience in studies of soft processes tells us that the real part of the zero angle scattering amplitude, provides us, through the dispersion representation with respect to the invariant energy of the collision, with information about the energy dependence of the cross section well beyond the energy where real part of amplitude is measured. The

reason for this is that  $\eta$ , the ratio of the real to imaginary part of the amplitude essentially measures the  $\ln s$  derivative of the cross section [1]:

$$\eta = \frac{\pi}{2} \frac{d \ln(F_2(x, Q^2))}{d \ln(1/x)}. \quad (1)$$

One can also use analyticity relations to derive a more accurate formula [2], leading to

$$\eta = \frac{s^\alpha}{\text{Im}A(s, t)} \tan \left[ \frac{\pi}{2} \left( \alpha - 1 + \frac{d}{d \ln s} \right) \right] \frac{\text{Im}A(s, t)}{s^\alpha}. \quad (2)$$

for  $F_2(x, Q^2) \propto x^{-\alpha}$ .

We propose a new methodology for investigating the energy dependence of hard processes through the real part of the amplitudes of high energy processes and also through the shapes of nondiagonal parton distributions. DVCS offers us a direct way to study of nondiagonal parton distributions. The idea is that at sufficiently small  $x$  the difference between diagonal and off-diagonal effects influences the  $x$  dependence of parton distributions only weakly. This has been known for a long time from calculations of Regge pole behaviour in quantum field theory. We also check that this statement is valid within the DGLAP approximation. Thus DVCS can be used to investigate asymptotia of parton distribution through the real part of the amplitude for DVCS.

Note that from a mathematical point of view, the actual extraction of nondiagonal parton distributions with the help of a factorization theorem from the data is not possible in DVCS due to the fact that the parton distributions depend on  $y_1$  and  $y_2 = y_1 - x$  which are dependent variables rather than independent as one would need and thus the inverse Mellin transform of the factorization formula cannot be found<sup>1</sup>. However, in practice, one will be able to neglect the dependence on  $y_2$  at sufficiently small  $x$  and by encoding the difference in the evolution of nondiagonal to diagonal distribution in a  $Q$ -dependent function, one can indeed extract the nondiagonal parton distribution at small  $x$  with an uncertainty associated with the  $Q$  dependent function.

---

<sup>1</sup>This is not true for diffractive di-muon production since there, we have two independent variables  $x$  and  $\xi_1$ , the longitudinal momentum fraction of the produced di-muon.

The major new result of our analysis is that the current successful fits to the  $F_{2N}(x, Q^2)$  HERA data lead to qualitatively different predictions for the asymmetry, reflecting different underlying assumptions of the fits about the behavior of parton densities at  $x$  below the HERA range. A recent analysis in Ref. [3] has shown that DVCS studies at HERA are feasible and we made predictions for the expected DVCS counting rate compared to DIS as well as the asymmetry  $A$  in the combined DVCS and Bethe-Heitler cross section for recent H1 data.

The paper is structured as follows. In Sec. II we review the necessary formulas of Ref. [3] for our analysis. In this context, the formula pertaining to the ratio of real to imaginary part of a scattering amplitude at small  $x$  is of particular importance. We then present the different fits to  $F_2(x, Q^2)$  in Sec. III and present the different results for the asymmetry  $A$  with respect to  $t$  and  $y$ , at fixed  $y$  and  $t$  respectively. Sec. V contains our conclusions and outlook.

## II. RELATIONS BETWEEN DVCS AND DIS

In order to compute the asymmetry  $A$ , we need the ratio of the imaginary part of the DIS amplitude to the imaginary part of the DVCS amplitude and the relative DVCS counting rate  $R_\gamma$ , expected at HERA in the interesting kinematic regime of  $10^{-4} < x < 10^{-2}$  and moderate  $Q^2$ , i.e. ,  $3.5 \text{ GeV}^2 < Q^2 < 45 \text{ GeV}^2$ . The relative counting rate  $R_\gamma$  is given by [3]

$$R_\gamma \simeq \frac{\pi\alpha}{4R^2Q^2B} F_2(x, Q^2)(1 + \eta^2). \quad (3)$$

where  $R$  is the ratio of the imaginary parts of the DIS to DVCS amplitude as given in [3]<sup>2</sup>,  $B$  is the slope of the  $t$  dependence (for more details see Ref. [3].) and  $\eta$  is the ratio of real to imaginary part of the DIS amplitude, i.e. ,  $F_2(x, Q^2)$ , given by Eq. (1).

We also need the differential cross section for DVCS which can be simply expressed

---

<sup>2</sup>We will use the results for  $R$  from [3] in our present analysis.

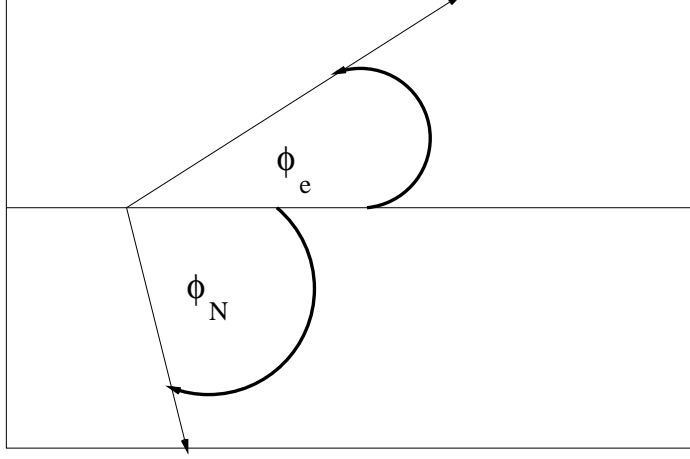


FIG. 1. The azimuthal final proton and electron angle in the transverse scattering plane.

through the DIS differential cross section by multiplying the DIS differential cross section by  $R_\gamma$  (see Ref. [3] for more details.) We then find using Eq. (3) for  $R_\gamma$

$$\frac{d\sigma_{DVCS}}{dx dy d|t| d\phi_r} = \frac{\pi\alpha^3 s}{4R^2 Q^6} (1 + (1 - y)^2) e^{-B|t|} F_2^2(x, Q^2) (1 + \eta^2) \quad (4)$$

with  $\sigma_{DVCS} = \frac{d\sigma_{DVCS}}{dt}|_{t=0} \times \frac{1}{B}$ . In writing Eq. (4) we neglected  $F_L(x, Q^2)$  - the experimentally observed conservation of s channel helicities in forward scattering high energy processes justifies this approximation - so that  $F_2 \simeq 2xF_1$ .  $y = 1 - E'/E$  where  $E'$  is the energy of the electron in the final state and  $\phi_r = \phi_N - \phi_e$ , where  $\phi_N$  is the azimuthal angle of the final state proton with respect to the reaction axis and  $\phi_e$  is the azimuthal angle of the final state electron (see Fig. 1).

In the case of Bethe-Heitler we find the differential cross section at small  $t$  to be

$$\frac{d\sigma_{BH}}{dx dy d|t| d\phi_r} = \frac{2\alpha^3 s y^2}{\pi t^2 Q^2} \left[ 1 - \frac{1}{1 - a \cos(\phi_r)} \right]^2 \left[ \frac{G_E^2(t) + \frac{|t|}{4m_N^2} G_M^2(t)}{1 + \frac{|t|}{4m_N^2}} \right], \quad (5)$$

with  $a^2 = 4y^2 |t| / (1 - y) Q^2$  and for  $-t \ll Q^2$  we can expand the first bracket in Eq. 5 and obtain the equation which we will use for the actual numerics. We find

$$\frac{d\sigma_{BH}}{dx dy d|t| d\phi_r} = \frac{8\alpha^3 s y^4}{\pi |t| Q^4 (1 - y)} \left[ \frac{G_E^2(t) + \frac{|t|}{4m_N^2} G_M^2(t)}{1 + \frac{|t|}{4m_N^2}} \right] \cos(\phi_r)^2, \quad (6)$$

with  $s$  being the invariant energy,  $y$  the energy fraction of the scattered electron/positron

and  $B$  the slope of the  $t$  distribution.  $G_E(t)$  and  $G_M(t)$  are the electric and nucleon form factors and we describe them using the dipole fit

$$G_E(t) \simeq G_D(t) = (1 + \frac{|t|}{0.71})^{-2} \quad \text{and} \quad G_M(t) = \mu_p G_D(t), \quad (7)$$

where  $\mu_p = 2.7$  is the proton magnetic moment. We make the standard assumption that the spin flip term is small in the strong amplitude for small  $t$ .

In order to write down the complete total cross section of exclusive photon production we need the interference term between DVCS and Bethe-Heitler. Since Bethe-Heitler amplitude is purely real, the interference term is only expressed through the real part of the DVCS amplitude. Note that in the case of the interference term one does not have a spinflip in the Bethe-Heitler amplitude, i.e. , one only has  $F_1(t)$ , as compared to Eq. (6) containing both spinflip and nonspinflip part , i.e. ,  $F_2(t)$ . The appropriate combination of  $G_E(t)$  and  $G_M(t)$  which yields  $F_1(t)$  is

$$\left[ \frac{G_E(t) + \frac{|t|}{4m_N^2} G_M(t)}{1 + \frac{|t|}{4m_N^2}} \right]. \quad (8)$$

We then find for the interference term of the differential cross section, where we already use Eq. 6,

$$\begin{aligned} \frac{d\sigma_{DVCS+BH}^{int}}{dx dy d|t| d\phi_r} = & \pm 2\eta \frac{\alpha^3 s y^2 F_2(x, Q^2) \cos(\phi_r) e^{-B|t|/2}}{R Q^5} \sqrt{\frac{2(1 + (1 - y)^2)}{|t|(1 - y)}} \\ & \times \left[ \frac{G_E(t) + \frac{|t|}{4m_N^2} G_M(t)}{1 + \frac{|t|}{4m_N^2}} \right]. \end{aligned} \quad (9)$$

where the  $+$  sign corresponds to electron scattering of a proton and the  $-$  sign corresponds to the positron. The total cross section is then just the sum of Eq. (4),(6),(9).

We define the asymmetry  $A$  as [3]

$$A = \frac{\int_{-\pi/2}^{\pi/2} d\phi_r d\sigma_{DVCS+BH} - \int_{\pi/2}^{3\pi/2} d\phi_r d\sigma_{DVCS+BH}}{\int_0^{2\pi} d\phi_r d\sigma_{DVCS+BH}}, \quad (10)$$

where  $d\sigma_{DVCS+BH}$  is given by the sum of Eq. (4),(6),(9). As explained in [3] this azimuthal angle asymmetry is due to the fact that the interference term in the combined DVCS and

Bethe-Heitler cross section is  $\propto \frac{p_t}{\epsilon}$ . Here  $p_t$  is the component of the final proton momentum transverse to the momentum of the initial electron and proton with  $\epsilon$  being polarization of the produced photon. Integrating over the upper hemisphere, from  $-\pi/2$  to  $\pi/2$ , one obtains a  $+$  sign from the interference term and a  $-$  sign from integrating over the lower hemisphere of the detector, from  $\pi/2$  to  $3\pi/2$ .

The real part of the DVCS amplitude is isolated through this asymmetry. Therefore, we investigate the influence of different  $F_2$  fits on the asymmetry through the relative counting rate which is directly sensitive to the ratio of real to imaginary parts of  $F_2$  as shown in Eq. (3).

### III. THE DIFFERENT FITS TO $F_2(X, Q^2)$

In the calculation of the asymmetry  $A$  we use the recent H1 data from Ref. [4] as previously used in Ref. [3], a logarithmic fit by Buchmüller-Haidt (BH) [5], the ALLM97 fit [6] and a leading order BFKL-fit [7] for illustrative purposes.

In the H1 data,  $F_2$  behaves for small  $x$  as  $x^{-\lambda}$  and hence  $\eta$  is just  $\frac{\pi}{2}\lambda$  where  $\eta^2 = 0.09-0.27$  in the  $Q^2$  range given in the previous section. Note that  $\eta$  has no  $x$  dependence, for small enough  $x$ , and thus depends only on  $Q^2$ . This is not true for all of the other fits.

$F_2$  in the BH fit <sup>3</sup> takes on the following form

$$F_2(x, Q^2) = 0.078 + 0.364 \log\left(\frac{Q^2}{0.5 \text{ GeV}^2}\right) \log\left(\frac{0.074}{x}\right), \quad (11)$$

and hence we find for  $\eta$

$$\eta = \frac{\pi}{2} 0.364 \frac{\log\left(\frac{Q^2}{0.5 \text{ GeV}^2}\right)}{F_2(x, Q^2)}. \quad (12)$$

---

<sup>3</sup>In a more recent fit Haidt [8] also used a double logarithmic fit with  $\log\left(\frac{Q^2}{Q_0^2}\right) \rightarrow \log\left(1 + \frac{Q^2}{Q_0^2}\right)$  being the essential difference, save some minor adjustments for some constants, in order to be able to describe more recent low  $Q^2$  data from HERA [9]. In the  $Q^2$  range considered in this analysis the difference is negligible.

Note that this  $\eta$  has not only the usual  $Q^2$  dependence but depends rather strongly on  $x$  also.

In the ALLM97 fit  $F_2$  at small  $x$  takes on the following form

$$F_2(x, Q^2) = \frac{Q^2}{Q^2 + m_0^2} (F_s^p(x, Q^2) + F_2^R(x, Q^2)), \quad (13)$$

where  $\eta$  is then given by

$$\eta = -\frac{\pi}{2} \frac{a_P c_P x_P^{a_P} + a_R c_R x_R^{a_R}}{c_P x_P^{a_P} + c_R x_R^{a_R}}. \quad (14)$$

The different variables and constants used in the fit can be found in [6].

In the case of the leading order BFKL approximation where  $F_2 \simeq x^{-\frac{4N_c \ln(2)\alpha_s}{\pi}}$ , we find  $\eta$  to be

$$\eta = \frac{\pi}{2} \frac{4N_c \ln(2)\alpha_s}{\pi}. \quad (15)$$

#### IV. RESULTS FOR THE ASYMMETRY $A$

In Fig. 2 - 4, we plot the asymmetry  $A$  as a function of  $t$  and  $y$  for fixed  $Q^2 = 12 \text{ GeV}^2$ , fixed  $y = 0.5$  and  $-t = 0.1 \text{ GeV}^{-2}$  and  $x = 10^{-4}, 10^{-3}, 10^{-2}$ . The slope  $B$  of the  $t$ -dependence for DVCS was taken to be  $B = 5 \text{ GeV}^2$  whereas for the Bethe-Heitler cross section we used the nucleon form factor as used in chapter 5. The counting rate  $R_\gamma$  was appropriately adjusted for the different fits according to Eq. (3). The solid curves in Fig. 2 - 4 are our benchmarks<sup>4</sup>.

Comparing the BH fit (medium-dashed curves), against our benchmarks we find a strong  $x$  dependence of the asymmetry in the BH fit as well as different shapes and absolute values.

---

<sup>4</sup>Though actual H1 data is used, we are still dealing with a leading order approximation and a particular model for the nondiagonal parton distributions at the normalization point was used in computing  $R_\gamma$  (see [3] for more details on the type of model ansatz and approximations used.).

As far as the ALLM97 fit is concerned (short-dashed curves), there is hardly a difference, as compared to the H1 fit in the asymmetry as a function of  $t$  and  $y$  in absolute value, shape and  $x$  dependence, except for  $x = 10^{-2}$  but this is due to the approximations we made for  $x_P$  and  $x_R$  which are not that good anymore at  $x = 10^{-2}$ .

If one compares the LO BFKL fit (long-dashed curves) to the H1 fit one sees immediately that the BFKL fit is totally off in almost all aspects and was only included here as an illustrative example.

## V. CONCLUSIONS

In the above we have shown the sensitivity of the exclusive DVCS asymmetry  $A$  to different  $F_2$  fits and made comments on the viability of each fit. Note that even a fit which reproduces  $F_2$  data, as well as its slope, in a satisfactory manner can be shown to lead to differences in the asymmetry shape. The sensitivity of the asymmetry to  $y$  and  $t$  will allow us, once experimentally determined, to make a shape fit and hence make a shape fit to nondiagonal parton distributions for the first time.

## ACKNOWLEDGMENTS

This work was supported under DOE grant number DE-FG02-93ER40771.



## REFERENCES

- [1] V.N.Gribov and A.A.Migdal, Yad.Fiz. 8(1968)1002 Sov.J.Nucl.Phys.8(1969)583.
- [2] J.B.Bronzan, Argonne symposium on the Pomeron, ANL/HEP-7327(1973)p.33;  
J.B.Bronzan, G.L.Kane, and U.P.Sukhatme, Phys. Lett. **B49** (1974) 272.
- [3] L. Frankfurt, A. Freund and M. Strikman, hep-ph/9710356 to appear In Phys. Rev. D. .
- [4] H1 Collaboration, Nucl. Phys. **B470**, 3 (1996).
- [5] W. Buchmüller and D. Haidt, hep-ph/9605428.
- [6] H. Abramowicz and A. Levy, hep-ph/9712415.
- [7] E.A. Kuraev, L.N. Lipatov, V.S. Fadin, Sov. Phys. JETP **45**, 199 (1977), Ya.Ya. Balitskii  
and L.N. Lipatov, Sov. J. Nucl. Phys. **28**, 822 (1978).
- [8] Proceedings of the 5th. International Workshop on Deep Inelastic Scattering and QCD,  
p. 386 (1997).
- [9] H1 Collaboration, Nucl. Phys. **B497**, 3 (1997).

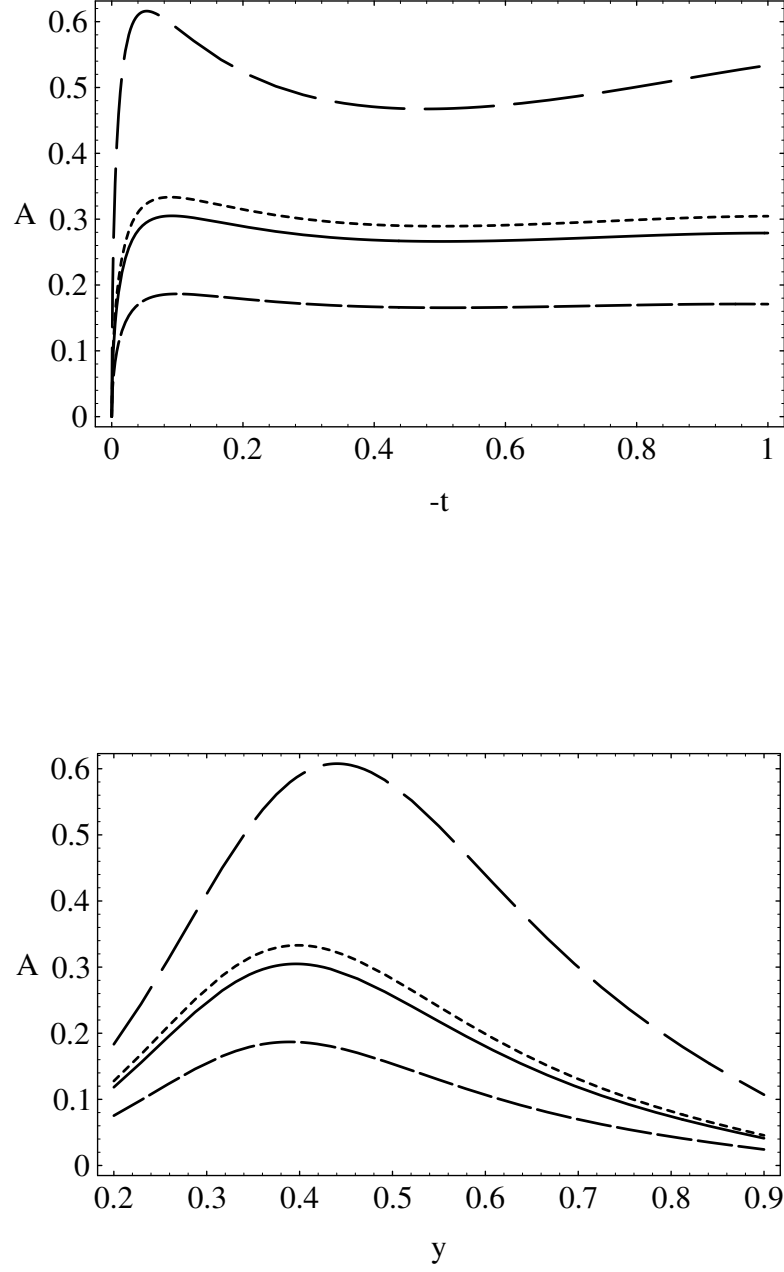


FIG. 2. H1 fit (solid curve), the Buchmüller fit (medium-dash curve), ALLM97 fit (short-dash curve) and BFKL fit (long-dash curve) for  $x = 10^{-4}$ . a) Asymmetry  $A$  versus  $t$  for fixed  $y = 0.4$ . b) Asymmetry  $A$  versus  $y$  for fixed  $-t = 0.1 \text{ GeV}^{-2}$ .

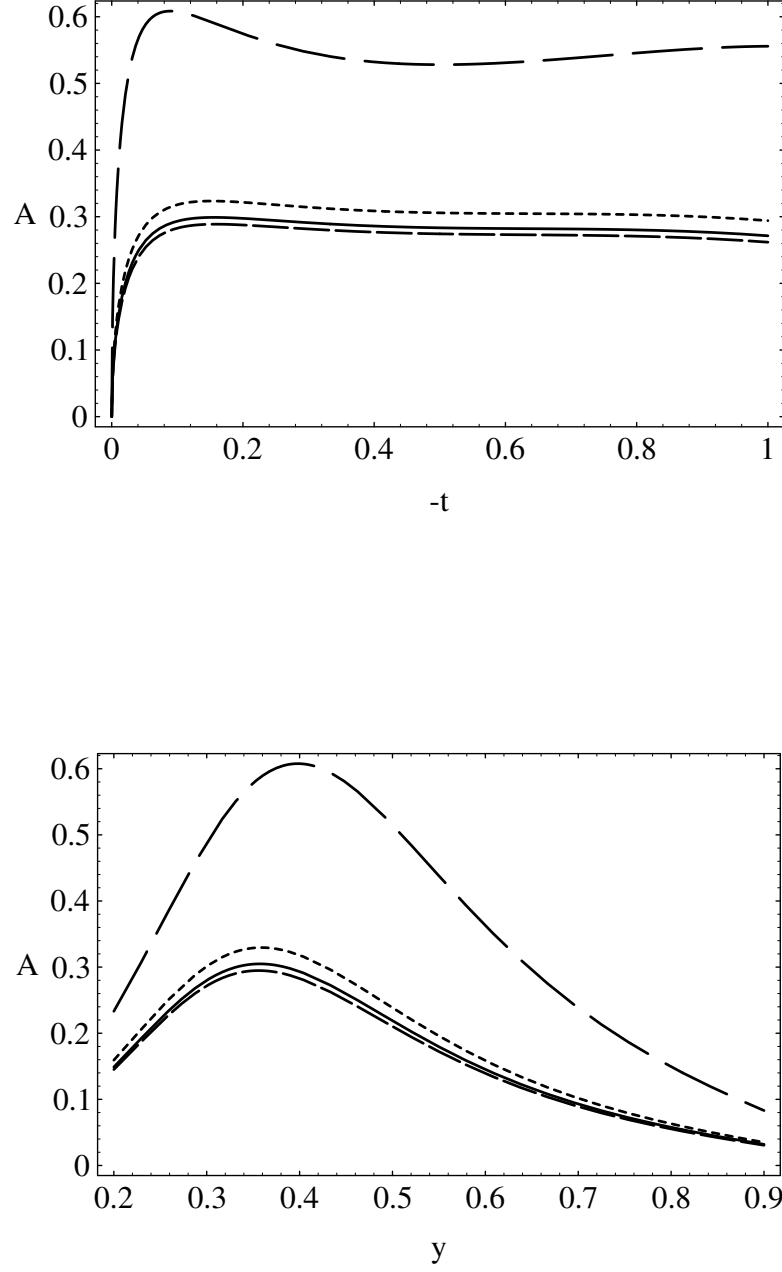


FIG. 3. H1 fit (solid curve), the Buchmüller fit (medium-dash curve), ALLM97 fit (short-dash curve) and BFKL fit (long-dash curve) for  $x = 10^{-3}$ . a) Asymmetry  $A$  versus  $t$  for fixed  $y = 0.4$ . b) Asymmetry  $A$  versus  $y$  for fixed  $-t = 0.1 \text{ GeV}^{-2}$

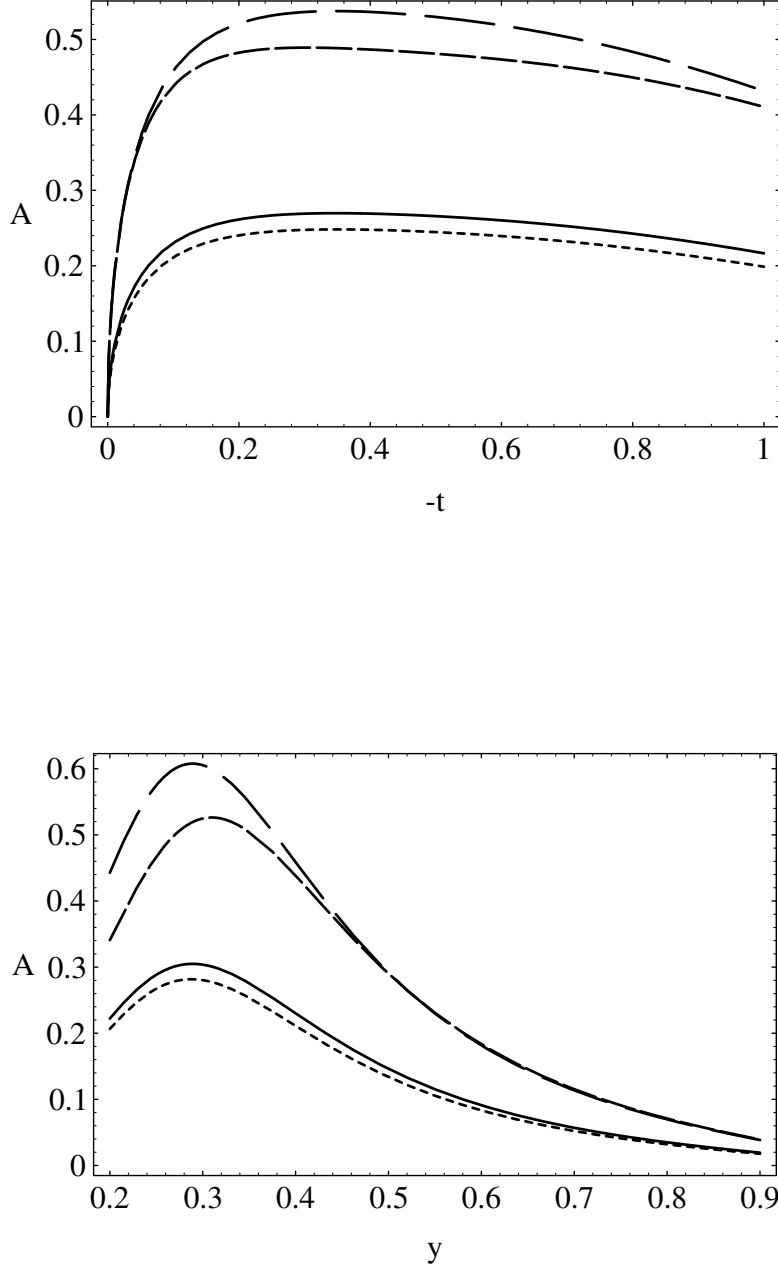


FIG. 4. H1 fit (solid curve), the Buchmüller fit (medium-dash curve), ALLM97 fit (short-dash curve) and BFKL fit (long-dash curve) for  $x = 10^{-2}$ . a) Asymmetry  $A$  versus  $t$  for fixed  $y = 0.4$ . b) Asymmetry  $A$  versus  $y$  for fixed  $-t = 0.1 \text{ GeV}^{-2}$